

SCIENTIFIC REPORTS



OPEN

MicroRNA-27a Induces Mesangial Cell Injury by Targeting of PPAR γ , and its In Vivo Knockdown Prevents Progression of Diabetic Nephropathy

Received: 16 July 2015

Accepted: 26 April 2016

Published: 17 May 2016

Lina Wu^{1,2}, Qingzhu Wang¹, Feng Guo¹, Xiaojun Ma¹, Hongfei Ji^{1,2}, Fei Liu¹, Yanyan Zhao¹ & Guijun Qin¹

MicroRNAs play important roles in the pathogenesis of diabetic nephropathy (DN). In this study, we found that high glucose upregulated miR-27a expression in cultured glomerular mesangial cells and in the kidney glomeruli of streptozotocin (STZ)-induced diabetic rats. miR-27a knockdown prevented high glucose-induced mesangial cell proliferation and also blocked the upregulation of extracellular matrix (ECM)-associated profibrotic genes. Reduction of cell proliferation and profibrotic gene expression by a miR-27a inhibitor depended upon the expression of peroxisome proliferator-activated receptor γ (PPAR γ). Further studies showed that miR-27a negatively regulated PPAR γ expression by binding to the 3'-untranslated region of rat PPAR γ . An antisense oligonucleotide specific to miR-27a (antagomir-27a) significantly reduced renal miR-27a expression in STZ-induced diabetic rats and significantly increased PPAR γ levels. Antagomir-27a also reduced kidney ECM accumulation and proteinuria in STZ-induced diabetic rats. These findings suggest that specific reduction of renal miR-27a decreases renal fibrosis, which may be explained in part by its regulation of PPAR γ , and that targeting miR-27a may represent a novel therapeutic approach for DN.

Diabetic nephropathy (DN) is a major microvascular complication of diabetes, and is the leading cause of end-stage renal disease. The key pathological hallmarks of DN are mesangial cell (MC) proliferation and an accumulation of extracellular matrix (ECM) proteins such as collagens and fibronectin. These processes are driven largely by the cytokine TGF- β 1¹⁻³. Despite substantial progress made in recent decades, our understanding of the underlying disease mechanisms is incomplete, and there is a need for identification of additional biomarkers and novel targets in order to improve DN treatment options.

MicroRNAs (miRNAs) are endogenously expressed, small noncoding RNAs that negatively regulate gene expression by binding to the 3'-untranslated region (3'-UTR) of target mRNAs⁴⁻⁶. miRNAs play important roles in cell growth, differentiation, proliferation, apoptosis, and cell death, and contribute to the pathogenesis of many human diseases, including cancer, diabetes, and diabetic complications such as DN in addition to other potential diseases⁷⁻⁹. The miR-27 gene family (miR-23a, 27a, and the 24-2 cluster) contributes to the regulation of cell cycle progression, proliferation, and hypertrophy¹⁰. Recently, Nielsen *et al.*¹¹ demonstrated that 12 human miRNAs, including miR-27a, were upregulated in the serum of patients with type 1 diabetes. miR-27a expression is also upregulated in both metabolic syndrome and type 2 diabetes, and there is a strong positive correlation between miR-27a and fasting glucose levels¹². In addition, miR-27a is upregulated in adipose tissue in a spontaneous rat model of type 2 diabetes mellitus, and its expression is increased in adipocytes in response to hyperglycaemia¹³. Collectively, these results suggest a role for miR-27a in the pathophysiology of type 1 and 2 diabetes. Moreover,

¹Division of Endocrinology, Department of Internal Medicine, The First Affiliated Hospital of Zhengzhou University, Zhengzhou, 450052, China. ²Institute of Clinical Medicine, The First Affiliated Hospital of Zhengzhou University, Zhengzhou, 450052, China. Correspondence and requests for materials should be addressed to G.Q. (email: hyqingj@zzu.edu.cn)

miR-27a is primarily expressed in adipose tissue, lung, heart, and kidney¹⁴, suggesting that it may play an important role in renal function. However, a role of miR-27a in DN has not been reported to date.

Peroxisome proliferator-activated receptor γ (PPAR γ), a potential target of miR-27a¹⁴, plays a critical role in ameliorating the course of DN^{15,16}. The 3'-UTR of PPAR γ contains a binding site for miR-27a, and miR-27a was reported to directly bind to PPAR γ mRNA and regulate adipocyte¹⁴ and human pulmonary artery endothelial cell¹⁷ differentiation. PPAR γ activation prevents high glucose (HG)-induced increases in TGF- β 1 expression¹⁸, modulates renal MC proliferation and differentiation¹⁹, and inhibits HG- or TGF- β 1-stimulated synthesis of type I collagen²⁰. However, it is unclear whether there is a functional interaction between miR-27a and PPAR γ with regard to MC proliferation or ECM deposition in DN.

In the current study, we found that miR-27a was upregulated in cultured glomerular MCs and in kidney glomeruli from streptozotocin (STZ)-induced diabetic rats. We also provide strong experimental evidence that miR-27a negatively regulates the expression of PPAR γ through the PPAR γ 3'-UTR. Moreover, our results confirmed that miR-27a downregulation increases PPAR γ expression, reduces MC proliferation and ECM accumulation, and ameliorates proteinuria. Thus, our results establish a critical role for miR-27a in the pathophysiology of DN.

Research Design and Methods

Reagents and antibodies. Streptozotocin (STZ) was supplied by Sigma (Saint Louis, MO, USA). Lipofectamine2000 was supplied by Invitrogen (Grand Island, USA). The miR-27a mimic, a miRNA negative control (NC mimic), miR-27a inhibitor, and miRNA inhibitor negative control (NC inhibitor) were designed and synthesized by GenePharma (Shanghai, PRC). Antagomir-27a, a specific PPAR γ small interfering RNA (siRNA), as well as a scrambled RNA (scRNA) were designed and synthesized by RiboBio (Guangzhou, PRC). The following antibodies were used: rabbit anti-rat polyclonal antibodies including anti-PPAR γ (Santa Cruz Biotechnology, CA), anti-TGF- β 1 and anti-PAI-1 (Cell Signaling Technology, USA), anti-GAPDH (CWBIO, Beijing, PRC), anti-collagen IV and anti-fibronectin (Bioss, Beijing, PRC).

Cell culture and transfection. The rat MC line (HBZY-1) was purchased from the Cell Culture Centre of the Institute of Biomedicine and Health (Guangzhou, PRC) and cultured as previously described²¹. Briefly, MCs were maintained at 37 °C in Dulbecco's modified Eagle's medium (Invitrogen, USA) supplemented with 10% foetal bovine serum (Gibco, USA) in an atmosphere containing 5% CO₂. Cells were treated with the indicated concentrations of glucose. Twenty-four hours prior to transfection, 2.0×10^5 MCs were plated into a 6-well plate. MCs were transfected using Lipofectamine2000 with final concentrations of 50 nM miR-27a mimic or miR-27a inhibitor and/or PPAR γ siRNA. The medium was replaced with fresh culture medium 4–6 h after transfection, and MCs were harvested for subsequent studies at 48 or 72 h after transfection.

Animal experiments. Eight-week-old male Sprague–Dawley rats (220 \pm 20 g) were purchased from the Experimental Animal Centre of Henan Province. All animal studies were approved by the Animal Care and Use Committee of the First Affiliated Hospital of Zhengzhou University and fully complied with the University guidelines for the care and use of laboratory animals. Diabetes was induced by a single intraperitoneal injection of 60 mg/kg STZ after fasting for 12 h. Blood glucose was measured to validate the induction of diabetes (>16.7 mmol/L) 72 h after STZ injection. Rats that received an injection of diluent buffer alone served as the normal control group (control, n = 5). Antagomir-27a or miR-27a mismatch mutations (NC antagomir) were administered to diabetic rats (n = 5, respectively) by intravenous injection at doses of 100 nM in 0.2 mL twice a week for 8 weeks. Body weight and blood glucose levels were monitored, and 24-h urine samples from each rat were collected every week. The rats were anesthetized with pentobarbital sodium (50 mg/kg body weight), and kidneys were harvested 24 h after the final injection. The kidney cortex was removed as described²², snap-frozen, and stored at –80 °C. Kidney glomeruli were isolated from cortical tissues by following a sequential sieving method²².

Quantitative real time (qRT)-PCR for miR-27a. miRNAs from cultured MCs and kidney glomeruli were isolated using the E.Z.N.A. miRNA Kit (Sigma, USA). cDNA was synthesized using miRNA-specific reverse transcription primers and the TaqMan MicroRNA Reverse Transcription Kit (Applied Biosystems, USA). miRNA-27a expression was quantified using miRNA-specific PCR primers and probe and the TaqMan Gene Expression Master Mix (Applied Biosystems, USA) on an Applied Biosystems 7500 Fast Sequence Detection System (Applied Biosystems). U6 small nuclear RNA (snRNA) served as an internal control and was amplified with forward (5'-ATTGGAACGATACAGAGAAGATT-3') and reverse (5'-GGAACGCTTCACGAATTTG-3') primers, and detected with a probe (5'-TGCGCAAGGATGACACGCA-3'). All primers and probes were obtained from GenePharma (Shanghai, PRC). Each sample was run in triplicate, and each experiment was repeated at least 3 times. Relative expression of miR-27a was analysed using the $2^{-\Delta\Delta CT}$ method²³.

Luciferase assays and site-directed mutagenesis. For luciferase assays, rat kidney MCs were cotransfected with the pEZX-MT05 vector with a PPAR γ -3'-UTR (GeneCopoeia RmiT049429-MT05) or a mut-PPAR γ -3'-UTR (GeneCopoeia CS-RmiT049429-MT05), the pEZX-MR03 vector encoding the miR-27a mimic (GeneCopoeia RmiR6129-MR03), and the pEZX-AM03 vector encoding the miR-27a inhibitor (GeneCopoeia RmiR-AN0359-AM03), using the EndoFectin Lenti Transfection Reagent (Cat.#: EFL1001-01, GeneCopoeia, Rockville, MD, USA). Following a 48-h transfection period, Gaussia luciferase (GLuc) and secreted alkaline phosphatase (SEAP) activities were measured using a Secrete-Pair Dual Luminescence Assay Kit (Catalogue # SPDA-D010, GeneCopoeia, Rockville, MD, USA) and a luminometer. SEAP activity was measured as an internal control. For each transfection, luciferase activities were averaged from 3 replicates.

RNA extraction and qRT-PCR. Total RNA was extracted from cultured MCs and kidney glomeruli using the Trizol reagent (TaKaRa Bio, Japan). First-strand cDNAs were synthesized using a cDNA Synthesis Kit

(TOYOBO, Japan) and then quantified by real-time PCR with the KOD SYBR Green qPCR Mix kit (TOYOBO, Japan) and appropriate primers. Reactions were performed on the ABI 7500FAST System (Foster City, CA). Relative gene expression levels were normalized to GAPDH expression. Primers were obtained from Sangon Biotech Co., Ltd. (Shanghai, PRC), and all primer information is available upon request.

Western blot analysis. Total protein was extracted from MCs and kidney glomeruli with a protein extraction reagent (Thermo, USA). Western blot analysis was performed as described previously²⁴. Membranes were exposed to a rabbit anti-PPAR γ antibody (diluted 1:100), or to a rabbit anti-TGF- β 1 or rabbit anti-PAI-1 antibody (diluted 1:1000). After incubation with the HRP-conjugated secondary antibody, blots were visualized with the Pierce ECL Western Blotting Substrate (Thermo Fisher Scientific, USA). Relative proteins expression levels were normalized to GAPDH levels.

Immunofluorescence microscopy. MCs were seeded onto chamber slides and transfected with the miR-27a mimic, the miR-27a inhibitor, or a negative control miRNA. At 48 h after transfection, cells were fixed in 4% paraformaldehyde solution for 20 min, permeabilized with 0.25% Triton X-100 for 15 min, and blocked with 1% BSA for 30 min at room temperature. After overnight incubation at 4 °C with a 1:50-diluted anti-PPAR γ antibody, MCs were exposed to a Cy3-labelled secondary antibody (diluted 1:500) for 1 h at room temperature, followed by DAPI staining for 2 min. The cellular distribution and localization of target proteins was examined under a fluorescent microscope (IX71; OLYMPUS, Japan).

Growth inhibition test. The Cell Counting Kit-8 (CCK-8) was employed to analyse cell proliferation, as described previously²⁵. MCs were plated at a density of 5,000 cells/well in 96-well plates, and subsequently transfected with the miR-27a inhibitor, PPAR γ siRNA, or negative controls at a final concentration of 50 nM. At 48 h after transfection, cell proliferation was measured with the CCK-8 Kit (BestBio, Shanghai, PRC). Each assay was performed with 6 replicates in 3 independent experiments.

Immunohistochemistry. Paraffin sections of rat kidneys were prepared by a conventional method and treated as we described previously²⁶. The anti-collagen IV and anti-fibronectin antibodies were diluted 1:100 and 1:200, respectively, for immunohistochemical staining experiments.

Light and electron microscopy. Kidney pathology in periodic acid-Schiff (PAS) and haematoxylin and eosin staining sections was examined by light microscopy. Glomerular area and mesangial expansion index were quantified using Image-Pro Plus 6.0 software. The renal cortex of kidneys was dissected into small pieces (1 mm³) and treated as we described previously²⁶. The ultrastructure of renal cortices was examined with an H-7500 transmission electron microscope (HITACHI, Japan).

Statistics. All data were analysed with SPSS 18.0 software (IBM, Endicott, NY, USA) and are presented as mean \pm S.E. Comparisons between more than 2 groups were assessed with one-way analysis of variance, followed by a Bonferroni test, and *P* values < 0.05 were considered statistically significant.

Results

Upregulation of miR-27a expression under hyperglycaemic conditions both *in vitro* and *in vivo*.

In vitro and diabetic animal model studies have confirmed the beneficial role of PPAR γ in diabetic kidney disease^{27,28}. To examine potential miRNAs that regulate PPAR γ expression, we utilized computational prediction programs (TargetScan, PicTar, miRanda, and miRGen) to identify potential binding sites for miRNAs in the PPAR γ -3'-UTR. This analysis indicated that miR-27a has a high probability of binding to the 3'-UTR of PPAR γ mRNA and that the putative miR-27a binding sites in the PPAR γ -3'-UTR are highly conserved between several mammals, such as humans, mice, rats, chickens, and dogs (Fig. 1A). Furthermore, miR-27a is highly expressed in the kidneys¹⁴, and is also upregulated in patients with type 1 or 2 diabetes^{11,12}. Thus, we focused on miR-27a in our experimental models, both *in vitro* and *in vivo*. As shown in Fig. 1B, miR-27a expression was significantly upregulated in rat kidney MCs exposed to HG (25 mM glucose). To examine the potential relevance of miR-27a upregulation in DN, we utilized a STZ-induced diabetes model in rats. As shown in Fig. 1C, miR-27a expression was significantly increased in the kidney glomeruli of diabetic rats. Taken together, these findings suggest that increased miR-27a levels may explain previously reported reductions of PPAR γ expression^{20,29}, which may in turn contribute to DN pathology.

PPAR γ is a target of miR-27a. To verify that miR-27a binds directly to the 3'-UTR of PPAR γ , we inserted the rat PPAR γ -3'-UTR (with the normal miR-27a binding site sequence or a mut-PPAR γ -3'-UTR) into the pEZ- γ -MT05 vector, which was then transfected into rat kidney MCs. As shown in Fig. 1D, miR-27a suppressed activity of the wild type PPAR γ -3'-UTR luciferase-reporter construct by 50% compared with cells cotransfected with a negative control. To determine the specificity of this result, MCs were cotransfected with the mutant PPAR γ -3'-UTR vector and the miR-27a overexpression vector in MCs. In this case, no significant changes in luciferase activity were observed upon overexpression of miR-27a or the negative control. Moreover, when the miR-27a expression vector was cotransfected with the miR-27a-inhibitor vector and the wild type PPAR γ -3'-UTR, the miR-27a inhibitor significantly counteracted miR-27a-mediated luciferase downregulation. These results clearly indicate that miR-27a directly specifically binds to the 3'-UTR of PPAR γ and suppress PPAR γ expression.

Inhibition of miR-27a suppressed HG-induced downregulation of PPAR γ in HG-treated MCs.

To confirm the impact of miR-27a on PPAR γ expression, MCs were transfected with a miR-27a mimic. As shown

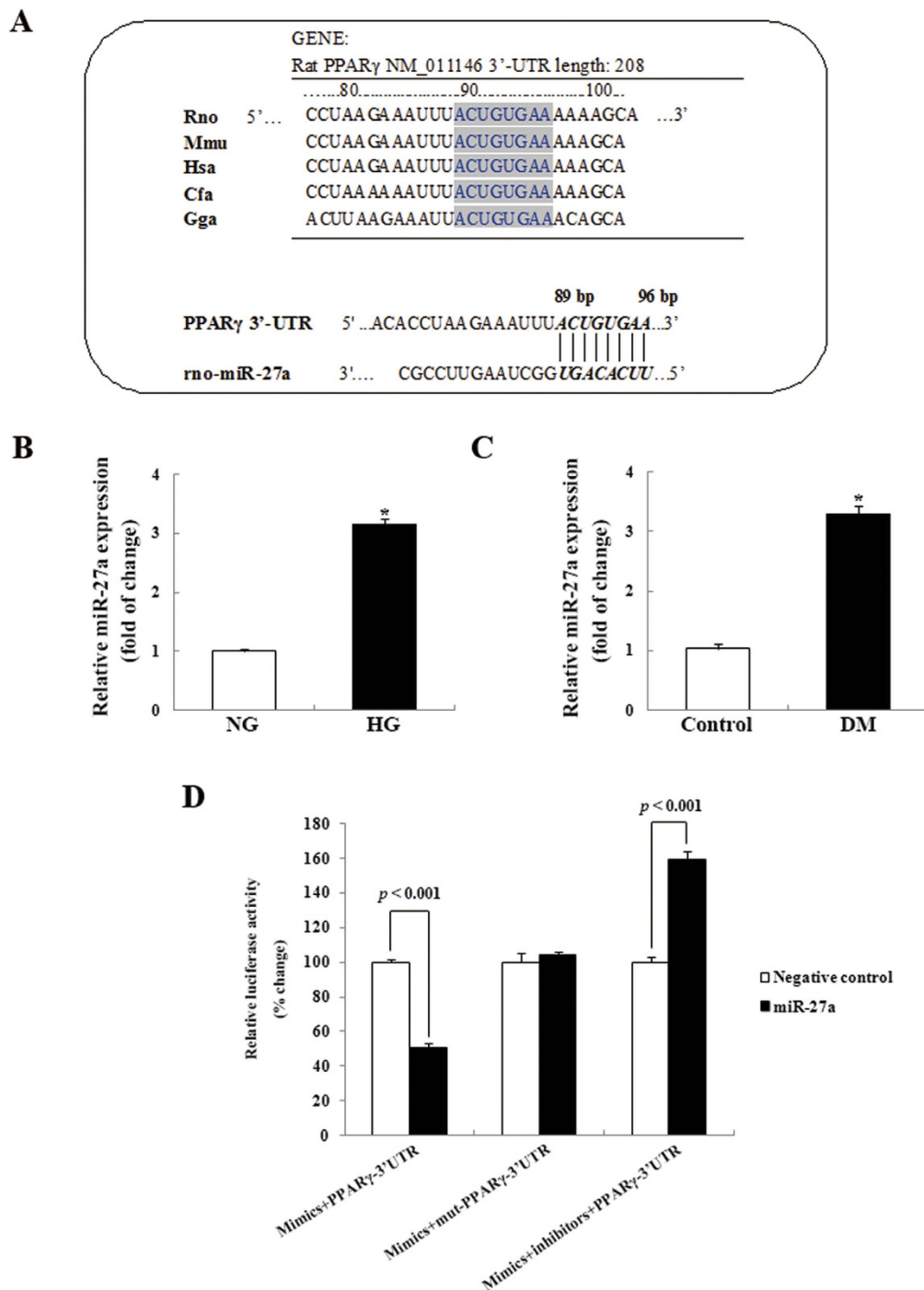


Figure 1. Expression of miR-27a is upregulated by high glucose, and targets the PPAR γ gene. (A) *Upper panel*, conservation of the miR-27a binding site in the 3'-UTR of mammalian PPAR γ genes. The miR-27a seed sequence is shown in the gray box. *Lower panel*, schematic illustration of miR-27a pairing with the rat PPAR γ 3'-UTR. Rno, *Rattus norvegicus*; Mmu, *Mus musculus*; Hsa, *Homo sapiens*; Cfa, *Canis lupus familiaris*; Gga, *Gallus gallus domesticus*; rno-miR-27a, *Rattus norvegicus*-miR-27a. (B) Real-time qPCR analysis showing miR-27a expression in rat kidney mesangial cells (MCs) treated with high glucose (HG, 25 mM) as compared with MCs treated with normal glucose (NG, 5.6 mM). miR-27a levels were normalized to U6 snRNA expression. Data are shown as mean \pm S.E. (n = 3). (C) Real-time qPCR analysis showing miR-27a expression in kidney glomeruli from streptozotocin-induced diabetic rats (DM) and normal control rats. miR-27a levels were normalized to U6 snRNA expression. Data are shown as mean \pm S.E. (n = 5). * $p < 0.05$ vs. NG; * $p < 0.05$ vs. control. (D) Rat kidney MCs were co-transfected with the pEZX-MT05 vector with a PPAR γ -3'-UTR or mut-PPAR γ -3'-UTR, and the indicated miR-27a mimic, inhibitor, or negative control. Following a 48-h transfection period, Gaussia luciferase (GLuc) and secreted alkaline phosphatase (SEAP) activities were measured. Each bar represents GLuc luciferase activity values normalized to those for SEAP activity, and the normalized values were expressed relative to MCs treated with the negative control miRNA. The results shown were obtained from 3 independent experiments.

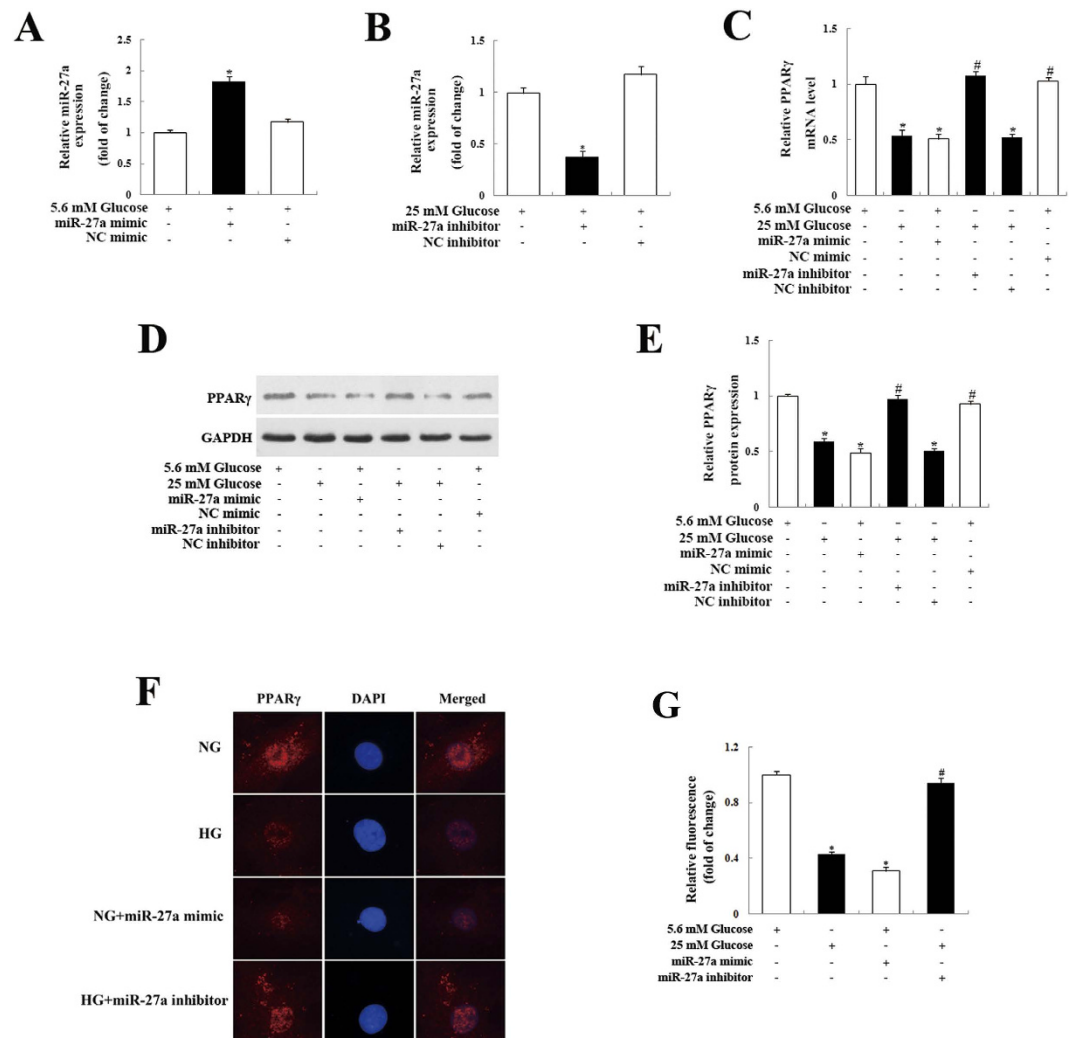


Figure 2. miR-27a negatively regulates PPAR γ expression. Rat kidney mesangial cells were transfected with a miR-27a mimic under normal glucose (NG, 5.6 mM) conditions or a miR-27a inhibitor under high glucose (HG, 25 mM) conditions. (A, B) At 48 h after transfection, real-time qPCR analysis was employed to detect alterations in miR-27a levels. miR-27a levels were normalized to U6 snRNA expression. (C) Real-time qPCR analysis of PPAR γ mRNA levels. (D) At 72 h after transfection, PPAR γ protein levels were detected by western blot analysis. GAPDH served as a loading control. (E) Densitometric analysis of the PPAR γ expression data shown in panel D. (F) Immunofluorescence detection of PPAR γ . Original magnification, $\times 400$. (G) Quantitative analysis based on PPAR γ fluorescence intensities. Data are shown as mean \pm S.E. (n = 3). * $p < 0.05$ vs. NG; # $p < 0.05$ vs. HG.

in Fig. 2, this lead to a clear increase in miR-27a levels in MCs (Fig. 2A) and a concomitant reduction in both PPAR γ mRNA (Fig. 2C) and protein (Fig. 2D,E) levels. We next examined whether a miR-27a inhibitor would have the opposite effect. We found that HG treatment significantly decreased PPAR γ mRNA (Fig. 2C) and protein (Fig. 2D,E) levels. Importantly, HG-induced downregulation of PPAR γ was reversed when MCs were transfected with a miR-27a inhibitor (Fig. 2B–E). To further examine the effect of miR-27a on PPAR γ , we performed immunofluorescence microscopy. Compared with normal glucose (NG)-treated MCs, PPAR γ immunofluorescence was significantly reduced in MCs transfected with the miR-27a mimic and treated with HG (Fig. 2F,G). In contrast, suppression of miR-27a activity with the miR-27a inhibitor increased PPAR γ immunofluorescence in HG-treated MCs (Fig. 2F,G). Taken together, these data indicate that miR-27a negatively regulates PPAR γ expression.

Inhibition of miR-27a attenuates MC proliferation and ECM accumulation. To determine the role of miR-27a in MC proliferation, we next examined cell viability. MC proliferation in the presence of HG was significantly increased compared with MCs cultured in NG conditions (Fig. 3A). In addition, the proliferation of miR-27a inhibitor-transfected MCs was significantly inhibited compared with HG-treated MCs and negative control cells. The result is in agreement with previous data showing that miR-27a downregulation suppresses cell growth *in vitro*³⁰. In contrast, when HG-treated MCs were transfected with both the miR-27a inhibitor and PPAR γ siRNA, the effect of miR-27a on cell growth was enhanced (Fig. 3A).

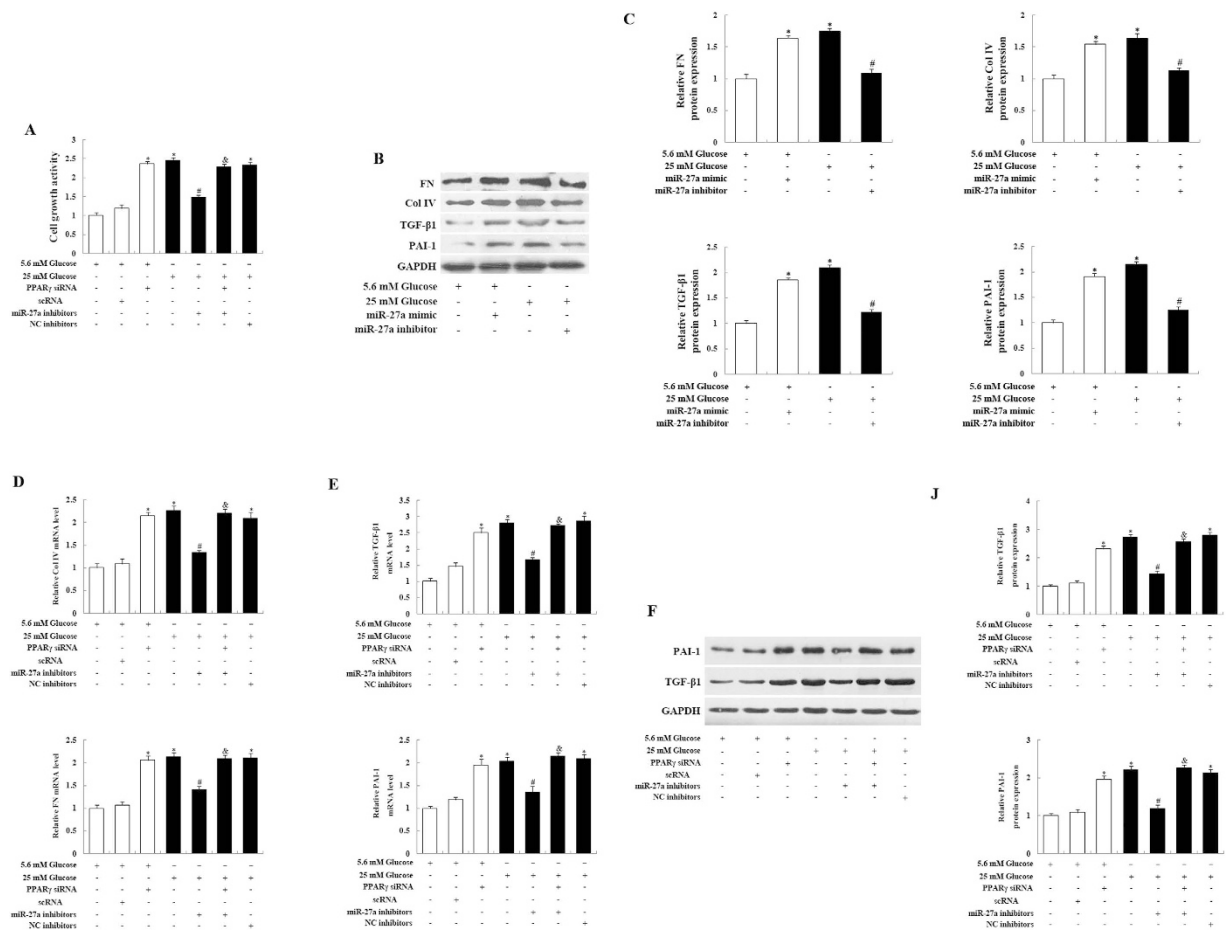


Figure 3. Downregulation of miR-27a with a miR-27a inhibitor prevented high glucose (HG)-induced mesangial cell (MC) proliferation and the expression of ECM-associated profibrotic genes via upregulation of PPAR γ expression. Rat kidney MCs were transfected with PPAR γ siRNA in the presence of NG levels (5.6 mM), or with a miR-27a inhibitor and/or PPAR γ siRNA in the presence of HG (25 mM). (A) Cell proliferation rates were determined using the CCK-8 assay. The results shown were obtained in 3 independent experiments and represent the mean \pm S.E. (B, C) Protein expression of collagen IV (Col IV), fibronectin (FN), TGF- β 1 and PAI-1 was detected by western blot analysis. GAPDH served as a loading control. Data are shown as mean \pm S.E. (n = 3). (D) Cellular expression of Col IV and FN was analysed by real-time qPCR, with normalization to GAPDH expression. Data are shown as mean \pm S.E. (n = 3). (E) Real-time qPCR analysis of TGF- β 1 and PAI-1 mRNA levels. Data are shown as mean \pm S.E. (n = 3). (F) TGF- β 1 and PAI-1 protein expression was detected by western blot analysis. GAPDH served as a loading control. (J) Densitometric analysis of the TGF- β 1 and PAI-1 expression data shown in panel F. Data are shown as mean \pm S.E. (n = 3). * p < 0.05 vs. 5.6 mM glucose; # p < 0.05 vs. 25 mM glucose; $\&$ p < 0.05 vs. 25 mM glucose + miR-27a inhibitor.

Because MCs contribute to the excessive accumulation of ECM proteins during DN, we next examined the effects of miR-27a on proteins relevant to this process. As shown in Fig. 3B,C, a marked increase in the protein levels of collagen IV, fibronectin, TGF- β 1 and PAI-1 were observed in the HG group compared with the NG group. As expected, miR-27a inhibitor suppressed the HG-dependent upregulation the levels of these ECM-associated profibrotic genes. In addition, upregulation of miR-27a by miR-27a mimic increased the levels of these profibrotic genes, compared with NG group. These data indicate that mimic and inhibitor of miR-27a had the opposite effect on ECM accumulation. HG also increased mRNA expression of collagen IV, fibronectin, TGF- β 1 and PAI-1 in MCs, as determined by qRT-PCR (Fig. 3D,E). However, the effect of HG was reversed by miR-27a inhibition. In contrast, the effect of miR-27a inhibitor was significantly decreased when HG-treated MCs were transfected with the miR-27a inhibitor and PPAR γ siRNA (Fig. 3D–J). PPAR γ activation is associated with reduced expression of ECM proteins and TGF- β 1 in the glomeruli of STZ-induced diabetic rats^{3,31} and may directly attenuate diabetic glomerular disease by inhibiting PAI-1 expression³². Together with our findings indicated that alterations in miR-27a levels could regulate PPAR γ levels (Fig. 2), these data demonstrate that HG-induced cell proliferation and ECM accumulation may be prevented by the inhibition of miR-27a, and that this is likely due to the consequent up-regulation of PPAR γ .

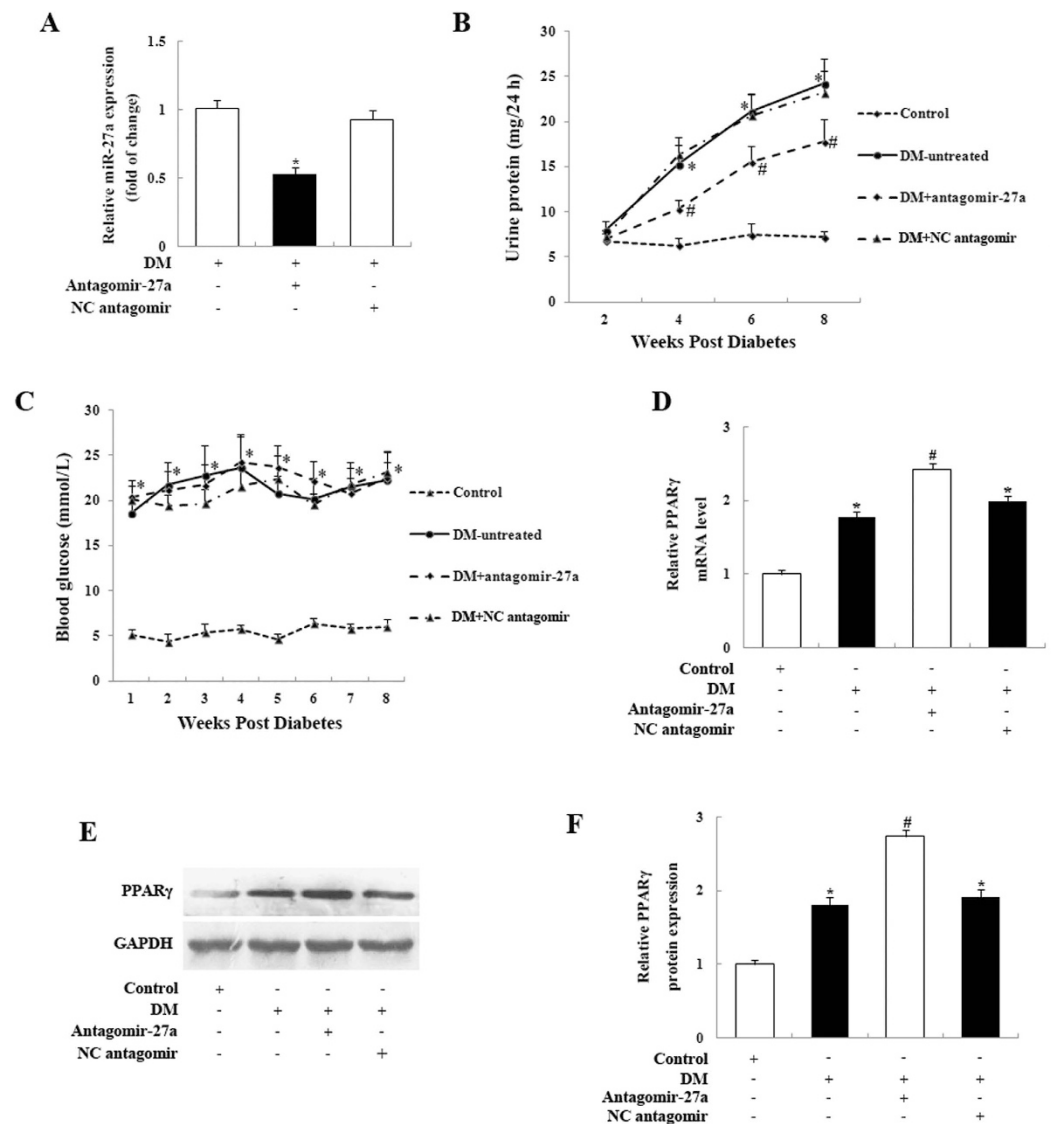


Figure 4. Inhibition of miR-27a with antagomir-27a reduces miR-27a expression, attenuates proteinuria, and increases PPAR γ expression in STZ-induced diabetic rats. (A) Real-time qPCR data showing significantly decreased miR-27a expression in the kidney glomeruli of antagomir-27a-treated diabetic rats, as compared with untreated diabetic rats (DM) or negative control rats. miR-27a levels were normalized to U6 snRNA expression. Data are shown as mean \pm S.E. (n = 5). (B) Injection of antagomir-27a led to improved proteinuria in STZ-induced diabetic rats (n = 5/group). (C) Blood glucose levels were not significantly affected by antagomir-27a treatment compared to untreated diabetic rats or negative control rats (n = 5/group). (D) Real-time qPCR analysis showed PPAR γ expression levels were significantly upregulated in the kidney glomeruli of antagomir-27a-treated diabetic rats, compared with untreated diabetic rats or negative control rats. Data are shown as mean \pm S.E. (n = 5). (E) Western blot analysis of PPAR γ protein expression in the kidney glomeruli of antagomir-27a-treated diabetic rats, compared with untreated diabetic rats or negative control rats. (F) Densitometric analysis of the PPAR γ expression data shown in panel E. Data are shown as mean \pm S.E. (n = 5). * p < 0.05 vs. Control; # p < 0.05 vs. DM.

Knockdown of miR-27a protects renal function in STZ-induced diabetic rats and ameliorates DN progression *in vivo*. Based on our *in vitro* data, we hypothesized that miR-27a inhibition *in vivo* might protect renal function in STZ-induced diabetic rats. Antagomirs, a novel class of chemically engineered oligonucleotides, are powerful functional inhibitors of miRNAs *in vivo*, and may represent a viable therapeutic strategy for silencing miRNAs in disease^{33–35}. To test whether they would be effective in DN, we used a chemically modified antisense oligonucleotide (antagomir-27a) to knock down miR-27a expression *in vivo*. As shown in Fig. 4A, miR-27a expression in kidney glomeruli was significantly suppressed in antagomir-27a-treated diabetic rats, compared with untreated diabetic rats. NC antagomir did not affect miR-27a levels in diabetic rats. We also found that proteinuria was significantly increased in untreated diabetic rats compared with normal control rats (Fig. 4B). After 8 weeks of antagomir-27a treatment, however, we observed a marked improvement in proteinuria

compared with untreated diabetic rats or negative control (NC antagomir) rats (Fig. 4B). However, blood glucose levels were not significantly affected by antagomir-27a (Fig. 4C). These results demonstrate that endogenous miR-27a levels are efficiently knocked down by antagomir-27a *in vivo*, and that this is associated with renoprotective effects in diabetic rats.

To determine the *in vivo* relevance of miR-27a knockdown on PPAR γ expression in the kidneys of STZ-induced rats, we examined the expression of PPAR γ mRNA and protein levels in the kidney glomeruli of antagomir-27a-treated rats. As shown in Fig. 4D–E, we confirmed that PPAR γ mRNA and protein levels were significantly increased following injection of antagomir-27a. We also found that PPAR γ mRNA and protein levels in the kidney glomeruli were increased in untreated diabetic rats compared with normal control rats, which is interesting given that the increase in PPAR γ during tissue injury may limit inflammation and injury responses³². To further validate the renoprotective effect of antagomir-27a, we examined the levels of key ECM-associated profibrotic genes, such as TGF- β 1, PAI-1, collagen IV, and fibronectin. In agreement with our *in vitro* results, the TGF- β 1 and PAI-1 levels were reduced in kidney glomeruli samples from antagomir-27a-treated diabetic rats (Fig. 5A–D). Furthermore, immunohistochemistry revealed that collagen IV and fibronectin levels were significantly attenuated in diabetic rats injected with antagomir-27a (Fig. 5E,F). These results demonstrate that the inhibition of endogenous miR-27a by antagomir-27a and subsequent increase in PPAR γ levels triggers the downregulation of several genes that play key profibrotic roles in diabetic rats.

To further validate our findings, we next examined the effect of antagomir-27a in the kidneys of treated rats by PAS and histopathological staining. This revealed an increased glomerular surface area, MC expansion, and thickened glomerular basement membranes in the kidneys of untreated diabetic rats. Conversely, renal pathology was ameliorated in diabetic rats injected with antagomir-27a (Fig. 6A–D). Moreover, electron microscopy revealed that podocyte morphology was severely compromised in both untreated diabetic rats and those treated with a negative control antagomir. In contrast, antagomir-27a ameliorated podocyte injury to some degree (Fig. 6E). These data further support the renoprotective effects of miR-27a inhibition in diabetic rats.

Discussion

Mounting evidence has implicated miRNAs in the development of DN. For instance, miR-192 levels are significantly increased in diabetic glomeruli, and this miRNA influences TGF- β -induced collagen 1- α 2 expression by downregulating E-box repressors³⁶. In addition, downregulation of miR-29c reduces podocyte apoptosis and decreases ECM protein accumulation, both *in vitro* and *in vivo*³⁷. miR-377 is upregulated in human and mouse MCs exposed to HG and indirectly stimulates increased fibronectin protein production³⁸. While miR-27a is reportedly upregulated in the serum of patients with type 1 or 2 diabetes^{11,12}, there have been no reports of pathological roles of miR-27a in DN to date. Here, we found that miR-27a expression was consistently upregulated in rat MCs exposed to HG and in kidney glomeruli from STZ-induced diabetic rats. Our results also indicated that miR-27a was capable of targeting the PPAR γ 3'-UTR to inhibit PPAR γ expression. Further, miR-27a upregulation led to enhanced cell proliferation and ECM accumulation through PPAR γ downregulation. Moreover, the *in vivo* inhibition of miR-27a protected diabetic renal function and ameliorated the progression of DN. Therefore, miR-27a is likely to be relevant in DN pathology, and is potentially an important therapeutic target for treating diabetic renal diseases.

Emerging evidence has suggested the importance of miR-27a overexpression in diabetes^{11–13}, although the full molecular mechanisms remain to be established. miR-27a is upregulated in cultured adipocytes exposed to hyperglycaemia¹³. Moreover, miR-27a levels are strongly and positively correlated with fasting glucose levels in patients with type 2 diabetes¹². Together, these findings indicate that increased miR-27a expression may be involved in the initial cellular responses to hyperglycaemia, which could eventually result in the development of diabetes. To determine whether miR-27a is a key regulatory factor in DN, we examined its levels in samples obtained from kidney glomeruli of STZ-induced diabetic rats and in kidney MCs exposed to hyperglycaemic conditions. Our integrated *in vitro* and *in vivo* studies indicated that miR-27a expression was significantly increased in these tissues and cell types. Importantly, inhibition of miR-27a with a miR-27a inhibitor *in vitro* or with antagomir-27a *in vivo* prevented HG-induced MC proliferation and ECM accumulation. Furthermore, antagomir-27a treatment significantly ameliorated proteinuria and renal pathology in STZ-induced diabetic rats. Although the regulatory influences of miR-27a remain incompletely defined, our data reveal that its overexpression clearly affects DN development.

Growing evidence indicates that PPAR γ activation is associated with the attenuation of DN. Our data showed that PPAR γ expression was decreased in kidney MCs exposed to hyperglycaemic conditions, which is in agreement with data in previous reports^{20,29}. Interestingly, the expression of miR-27a increased while PPAR γ expression decreased in HG-treated MCs. Recently, it was reported that miR-27a could directly bind to the 3'-UTR of PPAR γ mRNA and suppress PPAR γ expression, thereby suppressing adipocyte differentiation¹⁴. Similarly, miR-27a can bind to the PPAR γ 3'-UTR in human pulmonary artery endothelial cells and regulate cell proliferation¹⁷. Therefore, we hypothesized that increased miR-27a levels may provide the mechanistic explanation for reduced PPAR γ expression. We indeed confirmed that miR-27a bound to the PPAR γ 3'-UTR in rat kidney MCs. Furthermore, our results demonstrated that a miR-27a mimic significantly reduced PPAR γ expression in NG-treated MCs. Interestingly, we observed increased PPAR γ expression in the kidney glomeruli of diabetic rats, which was comparable to the upregulation seen in a study by Nicholas *et al.*³². PPAR γ upregulation may serve to limit injury responses in the kidneys of individuals with diabetes³². However, the increase in PPAR γ expression was insufficient to inhibit diabetic renal injury. Importantly, we showed that the knockdown of miR-27a with antagomir-27a significantly increased PPAR γ expression. Taken together, these results highlight miR-27a as an important regulator of PPAR γ expression in DN.

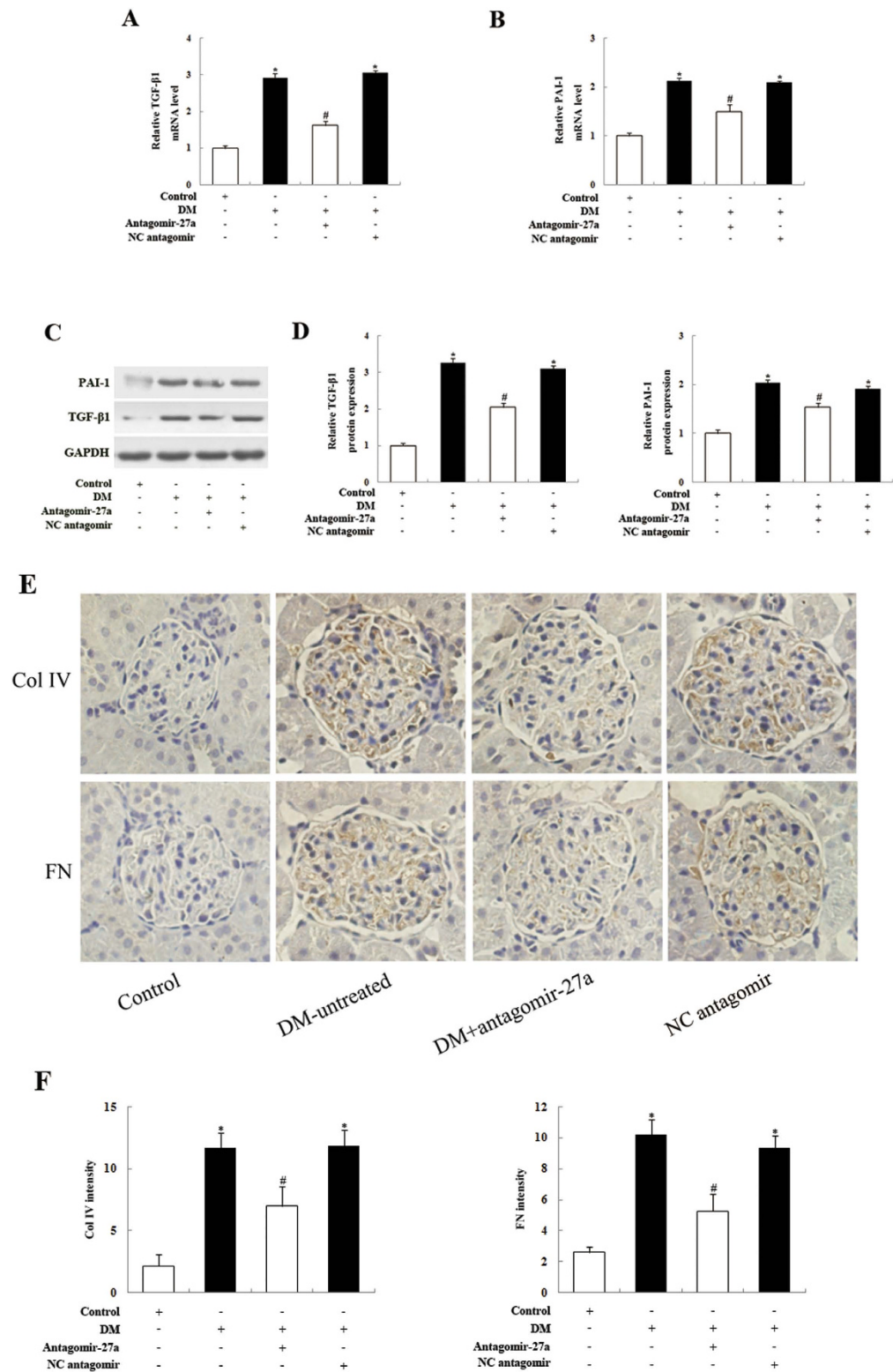


Figure 5. Inhibition of miR-27a with antagomir-27a reduces the expression of profibrotic genes and ECM proteins in the kidney glomeruli of STZ-induced diabetic rats. (A, B) Real-time qPCR analysis of TGF-β1 and PAI-1 expression in the kidney glomeruli of antagomir-27a-treated diabetic rats, compared with untreated diabetic rats or negative control rats. (C) Western blot analysis of TGF-β1 and PAI-1 protein expression in the kidney glomeruli of antagomir-27a-treated diabetic rats, compared with untreated diabetic rats or negative control rats. (D) Densitometric analysis of TGF-β1 and PAI-1 expression data shown in panel C. (E) Representative collagen IV (Col IV) and fibronectin (FN) immunohistochemistry staining of kidney sections in antagomir-27a-treated diabetic rats, compared with untreated diabetic rats or negative control rats. (F) Densitometry analysis of Col IV and FN. Data are shown as mean ± S.E. (n = 5). **p* < 0.05 vs. Control; #*p* < 0.05 vs. DM.

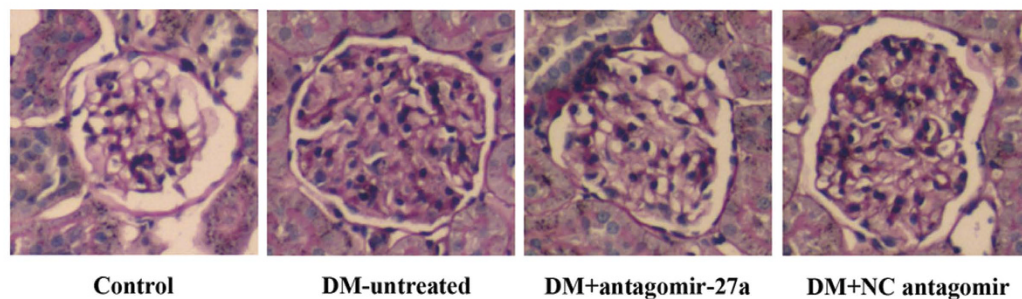
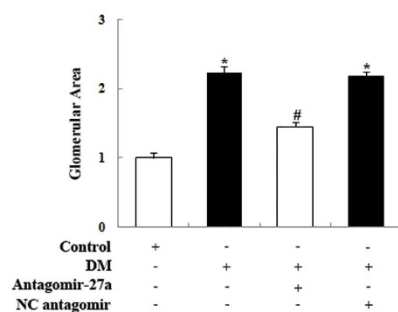
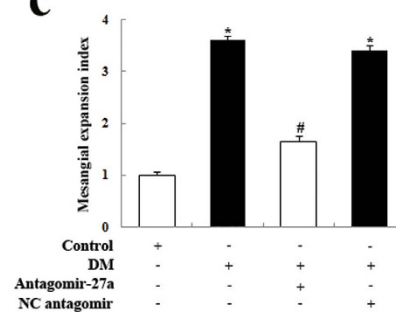
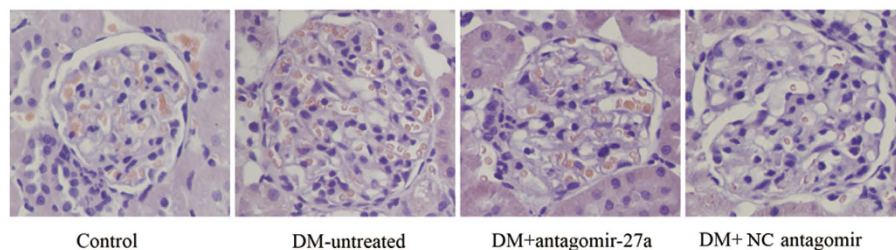
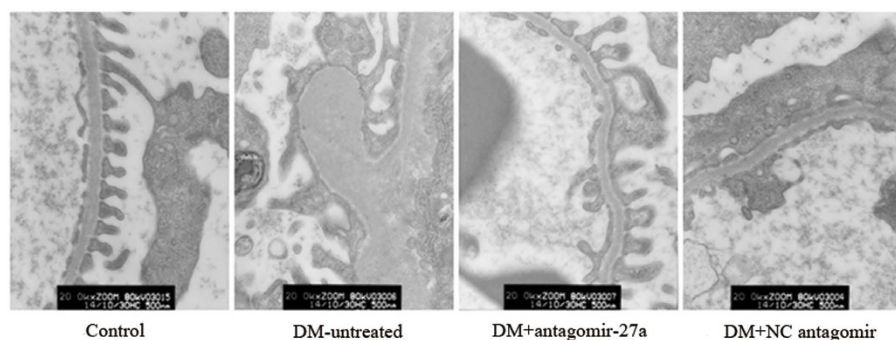
A**B****C****D****E**

Figure 6. Effect of antagomir-27a on renal morphology in STZ-induced diabetic rats. (A) Representative PAS staining of kidney sections in antagomir-27a-treated diabetic rats, compared with untreated diabetic rats or negative control rats ($\times 400$). (B) Glomerular area in PAS-positive sections. (C) Mesangial expansion index defined by the ratio of mesangial area/glomerular tuft area in PAS-positive sections. Data are shown as mean \pm S.E. * $p < 0.05$ vs. control; # $p < 0.05$ vs. DM. (D) Haematoxylin and eosin staining of rat glomeruli ($\times 400$). (E) Ultrastructure of kidneys from rats treated as indicated, as visualized under a transmission electron microscope ($\times 20,000$).

The pathological hallmark of diabetic glomerular lesions is ECM accumulation^{2,39}, and activation of PPAR γ can reduce MC proliferation and suppress ECM accumulation via inhibition of TGF- β 1 responses³, and by reducing PAI-1 expression³². Consistent with previous studies, our studies demonstrated that PPAR γ downregulation induced MC proliferation and increased levels of profibrotic genes in MCs exposed to hyperglycaemic conditions. In addition, the PPAR γ upregulation observed following miR-27a knockdown was associated with decreased MC proliferation and reduced expression of profibrotic genes. Importantly, knockdown of PPAR γ abrogated the

effects of miR-27a inhibitor on MC proliferation and profibrotic gene expression, indicating the critical role of PPAR γ as a target of miR-27a in both HG-induced cell proliferation and ECM accumulation in rat kidney MCs. Consistent with these *in vitro* results, there was a decrease in miR-27a expression and a corresponding increase in PPAR γ expression in antagomir-27a-treated diabetic rats; this reduced cell proliferation, and inhibited ECM accumulation compared with untreated diabetic rats and negative control rats. These data indicate that miR-27a negatively regulates PPAR γ , and in doing so, triggers enhanced MC proliferation and ECM accumulation.

Taken together, the data presented in this study reveal for the first time the critical role of miR-27a in the response of MCs exposed to HG concentrations. In addition, we show that miR-27a is a novel regulator of MC proliferation and ECM accumulation through the post-transcriptional regulation of PPAR γ . Furthermore, our data suggest that antagomir-based miRNA inhibitors (such as antagomir-miR-27a) can efficiently and specifically reduce renal miR-27a levels, renal hypertrophy, profibrotic gene expression, and renal fibrosis in diabetic rats. These findings provide new insights into the role of miR-27a in diabetes and indicate that miR-27a inhibitors may be useful for the treatment of DN.

References

1. Brosius, F. C., Khoury, C. C., Buller, C. L. & Chen S. Abnormalities in signaling pathways in diabetic nephropathy. *Expert. Rev. Endocrinol. Metab.* **5**, 51–64 (2010).
2. Mason, R. M. & Wahab, N. A. Extracellular matrix metabolism in diabetic nephropathy. *J. Am. Soc. Nephrol.* **14**, 1358–1373 (2003).
3. Tsuchida, K., Zhu, Y., Siva, S., Dunn, S. R. & Sharma, K. Role of Smad4 on TGF-beta-induced extracellular matrix stimulation in mesangial cells. *Kidney Int.* **63**, 2000–2009 (2003).
4. Bartel, D. P. MicroRNAs: genomics, biogenesis, mechanism, and function. *Cell* **116**, 281–297 (2004).
5. Ambros, V. The functions of animal microRNAs. *Nature* **431**, 350–355 (2004).
6. Farh, K. K. *et al.* The widespread impact of mammalian MicroRNAs on mRNA repression and evolution. *Science* **310**, 1817–1821 (2005).
7. Esquela-Kerscher, A. & Slack, F. J. Oncomirs - microRNAs with a role in cancer. *Nat. Rev. Cancer* **6**, 259–269 (2006).
8. Lagos-Quintana, M. *et al.* Identification of novel genes coding for small expressed RNAs. *Science* **294**, 853–858 (2004).
9. Xiao, C. & Rajewsky, K. MicroRNA control in the immune system: basic principles. *Cell* **136**, 26–36 (2009).
10. Chhabra, R., Dubey, R. & Saini, N. Cooperative and individualistic functions of the microRNAs in the miR-23a~27a~24-2 cluster and its implication in human diseases. *Mol. Cancer* **9**, 232 (2010).
11. Nielsen, L. B. *et al.* Circulating levels of microRNA from children with newly diagnosed type 1 diabetes and healthy controls: evidence that miR-25 associates to residual beta-cell function and glycaemic control during disease progression. *Exp. Diabetes Res.* **2012**, 896362 (2012).
12. Karolina, D. S. *et al.* Circulating miRNA profiles in patients with metabolic syndrome. *J. Clin. Endocrinol. Metab.* **97**, E2271–6 (2012).
13. Herrera, B. M. *et al.* Global microRNA expression profiles in insulin target tissues in a spontaneous rat model of type 2 diabetes. *Diabetologia* **53**, 1099–1109 (2010).
14. Kim, S. Y. *et al.* miR-27a is a negative regulator of adipocyte differentiation via suppressing PPAR γ expression. *Biochem. Biophys. Res. Commun.* **392**, 323–328 (2010).
15. Yang, J. *et al.* Role of PPAR γ in renoprotection in Type 2 diabetes: molecular mechanisms and therapeutic potential. *Clin. Sci.* **116**, 17–26 (2009).
16. Yang, J., Zhou, Y. & Guan, Y. PPAR γ as a therapeutic target in diabetic nephropathy and other renal diseases. *Curr. Opin. Nephrol. Hypertens.* **21**, 97–105 (2012).
17. Kang, B. Y. *et al.* Hypoxia mediates mutual repression between microRNA-27a and PPAR γ in the pulmonary vasculature. *PLoS One* **8**, e79503 (2013).
18. Okada, T. *et al.* Thiazolidinediones ameliorate diabetic nephropathy via cell cycle-dependent mechanisms. *Diabetes* **55**, 1666–1677 (2006).
19. Asano, T. *et al.* Peroxisome proliferator-activated receptor γ 1 (PPAR γ 1) expresses in rat mesangial cells and PPAR γ agonists modulate its differentiation. *Biochim. Biophys. Acta* **1497**, 148–154 (2000).
20. Zheng, F. *et al.* Upregulation of type I collagen by TGF-beta in mesangial cells is blocked by PPAR γ activation. *Am. J. Physiol. Renal Physiol.* **282**, F639–F648 (2002).
21. Kolavennu, V., Zeng, L., Peng, H., Wang, Y. & Danesh, F. R. Targeting of RhoA/ROCK signaling ameliorates progression of diabetic nephropathy independent of glucose control. *Diabetes* **57**, 714–723 (2008).
22. Xu, Z. G. *et al.* Relationship between 12/15-lipoxygenase and COX-2 in mesangial cells: potential role in diabetic nephropathy. *Kidney Int.* **69**, 512–519 (2006).
23. Livak, K. J. & Schmittgen, T. D. Analysis of relative gene expression data using real-time quantitative PCR and the 2^{- $\Delta\Delta$ CT} method. *Methods* **26**, 402–408 (2001).
24. Yang, F., Chung, A. C., Huang, X. R. & Lan, H. Y. Angiotensin II induces connective tissue growth factor and collagen I expression via transforming growth factor-beta-dependent and -independent Smad pathways: the role of Smad3. *Hypertension* **54**, 877–884 (2009).
25. Zhou, L. *et al.* Mechanism and function of decreased FOXO1 in renal cell carcinoma. *J. Surg. Oncol.* **105**, 841–847 (2012).
26. Wu, L., Zhang, Y., Ma, X., Zhang, N. & Qin, G. The effect of Resveratrol on FoxO1 expression in kidneys of diabetic nephropathy rats. *Mol. Biol. Rep.* **39**, 9085–9093 (2012).
27. Miceli, I. *et al.* Stretch reduces nephrin expression via an angiotensin II-AT(1)-dependent mechanism in human podocytes: effect of rosiglitazone. *Am. J. Physiol. Renal Physiol.* **298**, F381–F390 (2010).
28. Liang, Y. J. *et al.* L-165,041, troglitazone and their combination treatment to attenuate high glucose-induced receptor for advanced glycation end products (RAGE) expression. *Eur. J. Pharmacol.* **715**, 33–38 (2013).
29. Routh, R. E., Johnson, J. H. & McCarthy, K. J. Troglitazone suppresses the secretion of type I collagen by mesangial cells *in vitro*. *Kidney Int.* **61**, 1365–1376 (2002).
30. Kang, B.-Y. *et al.* Hypoxia mediates mutual repression between microRNA-27a and PPAR γ in the pulmonary vasculature. *PLoS One* **8**, e79503 (2013).
31. Zafriou, S. *et al.* Pioglitazone inhibits cell growth and reduces matrix production in human kidney fibroblasts. *J. Am. Soc. Nephrol.* **16**, 638–645 (2005).
32. Nicholas, S. B., Kawano, Y., Wakino, S., Collins, A. R. & Hsueh, W. A. Expression and function of peroxisome proliferator-activated receptor- γ in mesangial cells. *Hypertension* **37**, 722–727 (2001).
33. Krützfeldt, J. *et al.* Silencing of microRNAs *in vivo* with 'antagomirs'. *Nature* **438**, 685–689 (2005).
34. Esau, C. *et al.* miR-122 regulation of lipid metabolism revealed by *in vivo* antisense targeting. *Cell Metab.* **3**, 87–98 (2006).
35. Davis, S. *et al.* Potent inhibition of microRNA *in vivo* without degradation. *Nucleic Acids Res.* **37**, 70–77 (2009).

36. Kato, M. *et al.* MicroRNA-192 in diabetic kidney glomeruli and its function in TGF-beta-induced collagen expression via inhibition of E-box repressors. *Proc. Natl. Acad. Sci. USA* **104**, 3432–3437 (2007).
37. Long, J., Wang, Y., Wang, W., Chang, B. H. & Danesh, F. R. MicroRNA-29c is a signature microRNA under high glucose conditions that targets sprouty homolog 1, and its *in vivo* knockdown prevents progression of diabetic nephropathy. *J. Biol. Chem.* **286**, 11837–11848 (2011).
38. Wang, Q. *et al.* MicroRNA-377 is up-regulated and can lead to increased fibronectin production in diabetic nephropathy. *FASEB J.* **22**, 4126–4135 (2008).
39. Li, J. H., Huang, X. R., Zhu, H. J., Johnson, R. & Lan, H. Y. Role of TGF-beta signaling in extracellular matrix production under high glucose conditions. *Kidney Int.* **63**, 2010–2019 (2003).

Acknowledgements

This work was supported by grants from the National Natural Science Foundation of China (81400800 to X. Ma), the Innovation Scientists and Technicians Troop Construction Projects of Henan Province (134200510021 to G. Qin), as well as the Young Foundation of the First Affiliated Hospital of Zhengzhou University (to L. Wu). The authors appreciate the generous help from the Institute of Clinical Medicine (The First Affiliated Hospital of Zhengzhou University, Zhengzhou, China) in providing the necessary facilities. Dr. Guijun Qin is the guarantor of this work and, as such, had full access to all the data in the study and takes responsibility for the integrity of the data and the accuracy of the data analysis.

Author Contributions

G.Q., Q.W., X.M. and L.W. contributed to the study concept and design. L.W., F.G., H.J. and F.L. contributed to the data acquisition and analysis. L.W., F.G., G.Q., Q.W. and Y.Z. contributed to the interpretation of data and drafting of the manuscript. G.Q., Q.W., X.M., L.W. and Y.Z. performed critical revisions of the manuscript. All authors gave final approval of the version of the manuscript to be published.

Additional Information

Competing financial interests: The authors declare no competing financial interests.

How to cite this article: Wu, L. *et al.* MicroRNA-27a Induces Mesangial Cell Injury by Targeting of PPAR γ , and its In Vivo Knockdown Prevents Progression of Diabetic Nephropathy. *Sci. Rep.* **6**, 26072; doi: 10.1038/srep26072 (2016).



This work is licensed under a Creative Commons Attribution 4.0 International License. The images or other third party material in this article are included in the article's Creative Commons license, unless indicated otherwise in the credit line; if the material is not included under the Creative Commons license, users will need to obtain permission from the license holder to reproduce the material. To view a copy of this license, visit <http://creativecommons.org/licenses/by/4.0/>